05,11

Magnetic properties of Rb_2KFeF_6

© A.D. Balaev, V.N. Voronov, V.M. Sosnin, D.A. Balaev

Kirensky Institute of Physics, Federal Research Center KSC SB, Russian Academy of Sciences, Krasnoyarsk, Russia

E-mail: dabalaev@iph.krasn.ru

Received July 10, 2023
Revised July 10, 2023
Accepted July 16, 2023

The static magnetic properties of the Rb_2KFeF_6 single crystal in the temperature range $T = 1.8-300$ K in magnetic fields H up to 90 kOe are investigated. At $T > 1.8$ K the crystal is not magnetically ordered, however, the behavior of the inverse susceptibility $\chi^{-1}(T)$ indicates a negative paramagnetic Curie temperature of $\Theta \approx -0.8$ K. This is consistent with the analysis of the magnetization curve H_{eff} by replacing the external field with an effective H_{eff} field with a negative molecular field constant

Keywords: Rb_2KFeF_6 single crystal, magnetic properties, negative magnetic interactions.

DOI: 10.61011/PSS.2023.09.57114.143

1. Introduction

Rb_2KFeF_6 crystal structure is included in the elpasolite family — natural mineral — K_2NaAlF_6 with cubic sructure. General formula $A_2^+B^+M^{3+}X_6^-$ where A, B are alkali, M is a trivalent cation, X is a halogen. A variety of such compounds is known [1,2]. Beginning from the 70s of the past century until now, there have been a lot of studies addressing this family that were devoted to the synthesis, examination of X-ray diffraction and neutron diffraction data, thermophysical properties, theoretical symmetry analysis of structures, etc. Some of them are listed in [1–11]. With decreasing temperature, many elpasolite halides undergo structural phase transition from the highly symmetric cubic phase up to the monoclinic phase depending on the combination of shape and sizes of the cations and anions included in the general formula.

The examined Rb_2KFeF_6 crystal has cubic space group $Fm3m$ at room temperature with lattice parameter $a = 8.869$ Å [3]; phase transition temperature T_0 is ≈ 170 K [4–6]. In [7], detailed analysis was performed and hypothetic causes of phase transitions in elpasolites were described on the basis of cation size variation and entropy during phase transition. In [8], neuron diffraction data at 290 K and 10 K are reported, according to the data the crystal is assigned to cubic space group $Fm3m$ at $T > 170$ K, and has orthorhombic symmetry $Pmnn$ in the low temperature region. The structural transition with decreasing T according to [8] is caused by two factors: F^{1+} ordering with FeF_6 and KF_6 octahedra rotation, and Rb atom displacement.

Unfortunately, there is a relatively small body of literature that is concerned with the properties of elpasolites with paramagnetic trivalent ions. Studies [9,10] devoted to the investigation of susceptibility in compounds with trivalent $4f$-ions in ReF_6 octahedra. In [9], for compounds with Kramers Gd, Er, Yb ions, no magnetic ordering within the temperature range above 0.45 K was found and the inverse susceptibility behavior $\chi^{-1}(T)$ provides the paramagnetic Curie temperature ≈ 0 K. For non-Kramers $4f$-ions, Van Vleck behavior of the susceptibility-temperature dependence was detected. A well-defined Neel peak was found in Cs_2NaHoF_6 at $T_N = 0.62$ K. Findings similar to [9] were obtained for $Cs_2NaReCl_6$ systems (Re — rare earth element) in [10].

In [11], point defects (vacancies in place of M^{3+}) were found in perovskite-like crystals and investigated by the EPR method. It is shown that Rb_2KFeF_6 is paramagnetic at $T = 300$, 77 K with g-factor equal to 2.04. It is also noted that fluorine elpasolites are hydroscopic.

2. Single-crystal growth

RbF (C.P.), KF·HF, FeF_3 — (P) were used as primary components. Degassing of the prepared primary reagents was carried out in a vacuum drying oven at 500 K with residual pressure 0.1 Pa during 24 hours mainly for removal of the adsorbed and partially crystallization moisture. Rb_2KFeF_6 was synthesized in two stages: (1) by sintering stoichiometric compound followed by (2) melting and crystallization in platinum boats in argon atmosphere with 10 mol.% HF. Heating was carried out in a horizontal tube furnace with constant axial temperature gradient 25 K/cm, primary block growth rate was 3.5 mm/h. Transparent noncontaminated blocks were sampled and used for recrystallization.

Recrystallization was carried out by the Bridgman method without inocula in thick-wall platinum ampoules with a diameter of 10 mm and a wall thickness of 0.2 mm by decreasing oven temperature from (1373−1573) K to (773−923) K, where the first digit denotes the temperature in the beginning of the boat and the second figure shows the temperature in the end of the boat. Axial

temperature gradient in the crystallization zone 20 K/cm, crystallization rate 0.8 mm/h.

Single-crystal samples with edge dimensions up to 5 mm were prepared for the investigation. X-ray diffraction analysis at room temperature has shown conformity of the prepared Rb_2KFeF_6 single-crystals with cubic structure $Fm3m$ and lattice cell parameters $a = 8.869$ Å.

3. Crystal structure

Figure 1 shows the crystal structure at $T = 290$ K according to [8]. The crystal lattice cell contains four formula units. The Figure shows that there are two kinds of ion groups — FeF_6 and KF_6 octahedra. These octahedra have common vertices, alternate and form chains along three tetrad axes. Adjacent chains are also connected by vertices and form {100} type layers. Adjacent layers are displaced relative to each other by lattice half-spacing. Each of eight Rb^{1+} ions with positions 1/4, 1/4, 1/4 are in the centers of cubooctahedra with twelve vertices formed by F^{1+} ions. The main interatomic spacings are shown in the Figure. The data for parameters for low temperature are given in the discussion (Section 5).

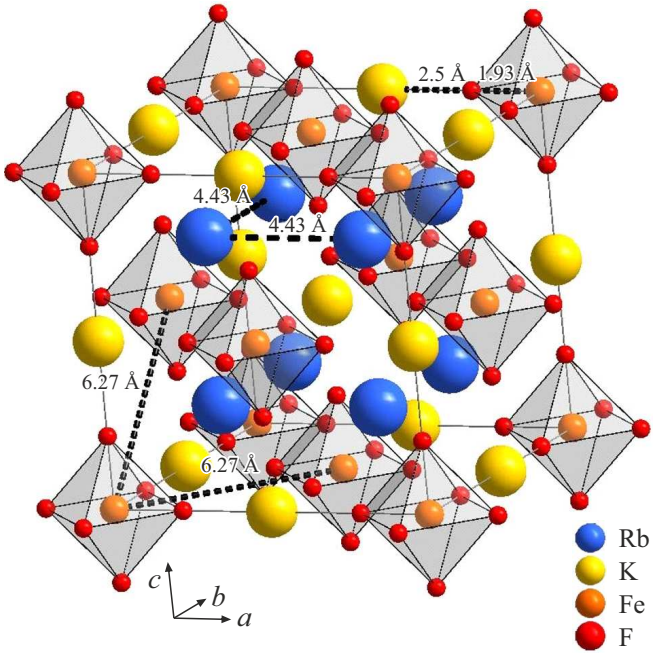

Figure 1. Rb_2KFeF_6 crystal structure at $T = 290$ K.

4. Magnetic measurements

Static magnetic properties of the Rb_2KFeF_6 single-crystal were measured using a vibrating magnetometer (hereinafter referred to as VSM) with a superconducting solenoid [12] in the temperature range from 4.2 to 300 K in magnetic fields up to 80 kOe, and PPMS-9 (Quantum Design) system in the temperature region from 1.8 to 300 K in fields up to 90 kOe.

The sample is mainly a $\sim 2.5 \times 3.5 \times 4.5$ mm rectangular parallelepiped with edges parallel to the tetrad axes. In addition, the crystal had one more natural face — $\sim 2 \times 2$ mm (110) type plane. The sample was adhered to a quartz pad with its appropriate face in such a way that the field H was perpendicular to this face. The magnetic field H direction was referred to the crystal axes for the cubic phase $Fm3m$.

Temperature dependence of magnetization $M(T)$ was measured within 4.2–300 K in field $H = 1$ kOe parallel to [100] along one of the axes C_4. By building molar susceptibility $\chi(T)$ and its reciprocal $\chi^{-1}(T)$, paramagnetic Curie temperature Θ equal to ≈ -0.5 K and effective magnetic moment μ_{eff} of the Fe^{3+} atom ($\mu_{\text{eff}} \approx 5.9\mu_B$ were determined, where μ_B is the Bohr magneton). To reverify the negative value of Θ, $M(T)$ were measured at H parallel to the same direction as well as to the other two axes C_4. $M(T)$ dependence was also measured at field **H** direction perpendicular to the natural face — (110) type plane — i.e. at **H** $\parallel$ [110]$-C_2$ and **H** $\parallel$ [101]. All three measurements were shown in Figure 2. It is shown that $\chi(T)$ for all directions are hyperbola and $\chi^{-1}(T)$ are straight lines. Thus, he Curie–Weiss law is fulfilled

$$\chi(T) = C/(T - \Theta),$$

where $\Theta = \lambda_T C$, C is the Curie constant, λ_T is the molar mean-field constant [13,14].

The inset in Figure 2 shows the behavior of $\chi(T)$ for **H** directions parallel to axes C_4. At $T_0 \approx 170.5$ K, the start of a feature in $\chi(T)$ behavior can be seen that is indicative of the phase transition [4,5,7]. In the experiment, the temperature increases with the rate shown in the Figure. Within $170.5 \leq T \leq 173$ K, the magnetization remains almost constant. This is possible at a constant temperature of the sample, i. e. heat absorption by the sample is exhibited. Since latent heat of transition is detected, this transition shall be treated as kind I transition. It should be noted that below and above T_0, the magnetic state was unchanged. This is evident from the absence of a jump of $\chi(T)$ or of an inclination variation in $\chi^{-1}(T)$ at $T = 170.5$ K (Figure 2).

Figure 2 (except the inset) contains seven almost undistinguishable dependences containing up to 7000 experimental points in each. Final quantitative processing of $\chi^{-1}(T)$ for each direction with several test runs (for **H** $\parallel$ [100] direction — marked as 1-st, 2-nd and 3-d run) by least-square linear regression is presented in the Table. The Table also shows the obtained effective magnetic moments μ_{eff} and λ_T — molar mean-field constant. Mean-field constants per Fe^{3+} ion — λ_{T1}, required below for comparison with the equivalent quantity obtained from the $M(H)$ measurements are shown in the last table line.

The Table shows that there is some Θ, μ_{eff} and λ_T scatter. From our point of view this is shall be attributable

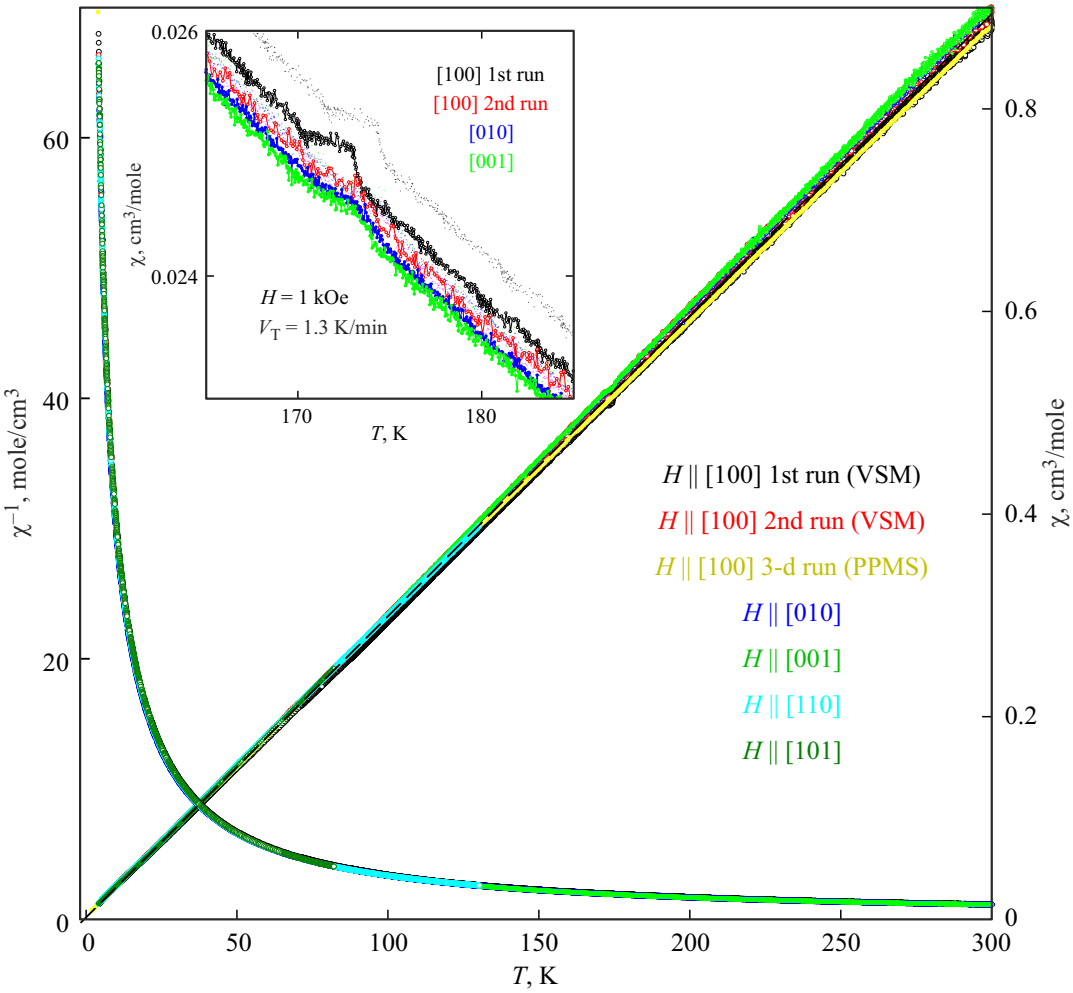

Figure 2. Temperature dependences of susceptibility $\chi(T)$ (righthand axis y) and reciprocal $\chi^{-1}(T)$ (lefthand axis y) of the Rb_2KFeF_6 single-crystal in the field $\mathbf{H} = 1$ kOe parallel to the directions shown in the Figure. Experiment — symbols with colors corresponding to various directions. The dashed line was plotted by given $\mathbf{H} \parallel [100]$ using the least-square method. Inset — similar behavior of $\chi(T)$ in the phase transition region.

Paramagnetic Curie temperature Θ, effective magnetic moment μ_{eff} and λ_T, λ_{T1} — mean-field constant obtained from $M(T)$ measurements for various (including repeating) directions of the Rb_2KFeF_6 crystal

System	PPMS	VSM					
Temperature range, K	1.8–300	4.2–300				4.2–130	4.2–80
Direction**H** $\parallel$	[100]	[100]	[100]	[010]	[001]	[110]	[101]
Θ, K	−1.25	−0.45	−0.87	−0.9	−0.47	−1.1	−0.81
μ_{eff}, μ_B	5.93	5.91	5.87	5.865	5.85	5.9	5.87
λ_T, cm^{-3}	−0.28	−0.16	−0.2	−0.207	−0.11	−0.25	−0.19
λ_{T1}, Gs	−1560	−897	−1125	−1160	−630	−1415	−1045

to the measurement error, rather than to the anisotropy of these values. This error includes not only the temperature measurement error, but also the accurate absolute magnetic moment (two systems were used for the study), external field, sample weight, and the effect of the demagnetizing factor of the sample for various directions. It should be noted that after two weeks of the study, crystal cloudiness and loose crystal surface were observed, and similar

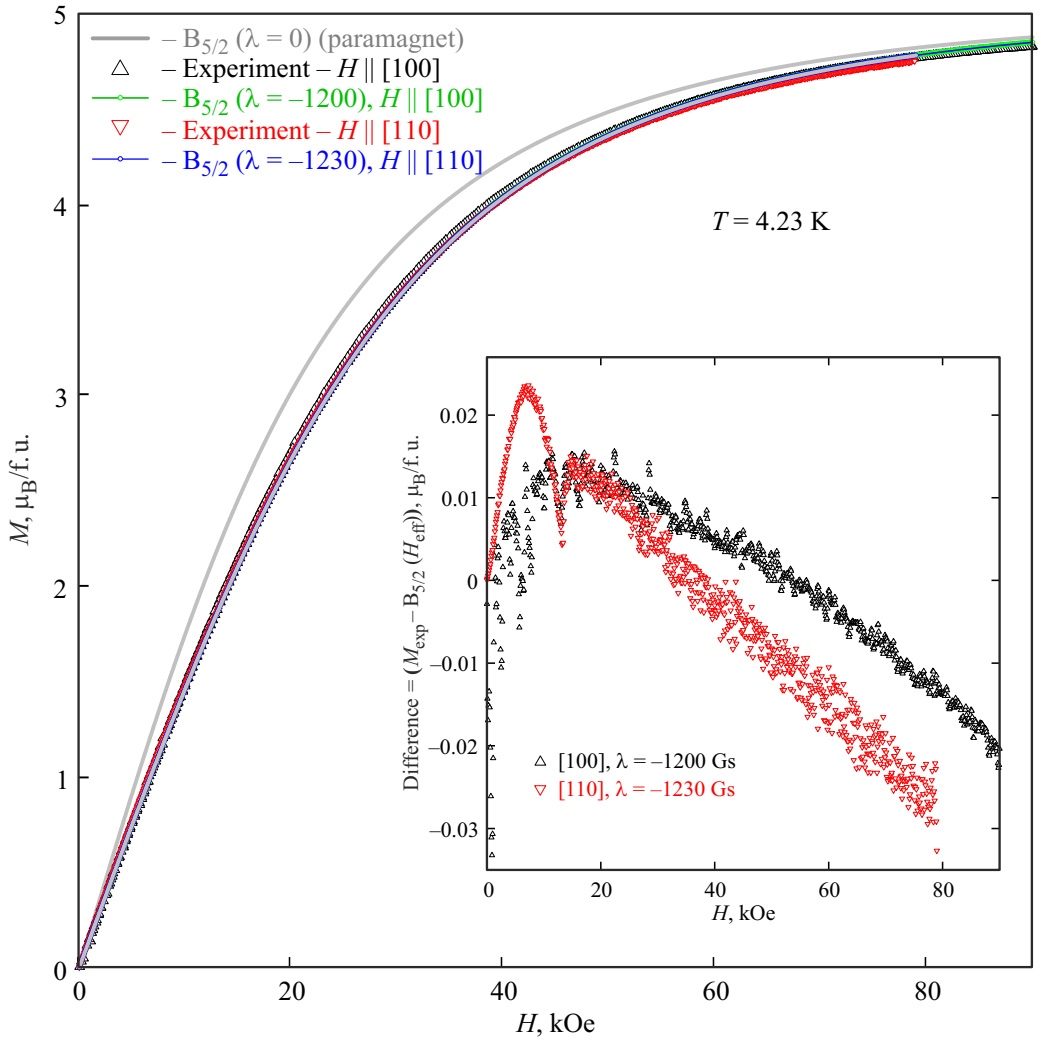

Figure 3. Dependences of the magnetization on the external field $M(H)$ of the Rb_2KFeF_6 single-crystal at the specified directions; $T = 4.23$ K. Symbols — experiment, solid curves — the Brillouin function $B_{5/2}(\lambda = 0)$ and fitting results within the mean-field theory (see the text in Section 4) — $B_{5/2}(\lambda \neq 0)$ for the mutual orientations of the external field **H** and crystallographic directions as specified in the legend. Inset: difference between the experiment and theory in terms of the Bohr magneton depending on H.

behavior was noted in [11]. In [3] it is pointed out that single-crystal destruction occurs during the phase transition that probably causes the visible degradation for the crystal after repeated temperature cycling during measurements.

Finally, the study of the magnetization-temperature dependences for various directions of the Rb_2KFeF_6 crystal shows that within $1.8 \leq T \leq 300$ K magnetic ordering is not observed and there is no $\chi(T)$ anisotropy for various directions. Inverse susceptibility dependences $\chi^{-1}(T)$ — are linear temperature functions, i. e. the Curie–Weiss law is fulfilled; negative Curie temperature (average) $\Theta \approx -0.83 \pm 0.25$ K is indicative of minor negative interaction between Fe^{3+} ions; effective magnetic moment (average) $\mu_{eff} = 5.89\,\mu_B$ is close to the theoretical value for Fe^{3+} ion in S state equal to $5.916\,\mu_B$; at $T_0 \approx 170.5$ K, response of kind I structural phase transition was detected.

To confirm negative interaction between Fe^{3+} ions in the crystal, studies of dependence of magnetization on the field $M(H)$ were carried out. In Figure 3, symbols show the experimental behavior of $M(H)$ in **H** || [100] and **H** || [110] directions at $T = 4.23$ K. No anisotropy occurs in the field behavior in these directions. The same figure shows the field dependence of magnetization for paramagnet $M(H) = M_0 B_{5/2}(x)$ (solid line) in accordance with the Brillouin function $B_{5/2}(x)$ at $x = gS\mu_B H/kT$. Here, $M_0 = gS\mu_B$ is the saturation magnetic moment per Fe^{3+} ion, g-factor equal to 2, $S = 5/2$ is the spin, k is the Boltzmann constant. It can be seen that the simple paramagnet model does not describe the experimental dependences.

To explain the experiment, approximation of two sublattices was taken [13], where the external field H is replaced by the effective field: $H_{eff} = H + \lambda M$, where λ is the mean-field constant, M is the magnetization in the external

field H. $M(H) = M_0 B_{5/2}(H_{\text{eff}})$ obtained in conditions of the best description of the experimental data are shown in Figure 3. Very close agreement with the experiment may be confirmed with varying only one adjustable parameter — λ (g-factor is assumed equal to 2 [11], $S = 5/2$). λ values for $\mathbf{H} \parallel [100]$ and [110] directions were chosen such that the positive and negative deviation of the difference between the experiment and theory (shown in Detail in Figure 3) from the zero line was approximately the same throughout the external filed range. Maximum discrepancy does not exceed $\sim 0.5\%$. λ values are shown in Figure 3, they are negative (similar to λ_{T1} and λ_T, see the Table) and differ slightly for various directions.

5. Discussion of findings

Magnetic measurements gave negative values of Θ from $M(T)$ and negative values of λ from $M(H)$. This is indicative of the negative interaction between Fe^{3+} ions. Value (average) of λ_{T1} (≈ 1120 Gs — see the last line of the Table) obtained from the $M(T)$ measurements is slightly lower than that of λ ($\approx -1200-1230$ Gs) obtained from $M(H)$ (Figure 3).

It should be noted that at $T < 170$ K in phase transition, lattice cell parameters vary very significantly in the ab plane and slightly (in the third decimal place) along the c axis. Whereby, for the low-temperature phase, according to [7], lattice constants at $T = 10$ K are $a = 6.157$ Å, $b = 6.151$ Å, $c = 8.894$ Å. In [4,5] it is shown that at $T < 170$ K the Bravais lattice is of P — type that is $I4/mmm$ or $I4/m$ subgroup. For qualitative assessment of the interaction energy and distance between Fe^3 ions, it is sufficient to represent the Bravais lattice as pseudotetragonal with $I4/m$ symmetry and $a \approx b \approx a^{\text{cub}}/\sqrt{2}$, $c \approx c^{\text{cub}}$ [4]. It may be assumed that the crystal axes a and b during structural transition rotate around the c axis at 45°. Moreover, for the low-temperature phase, according to [8], Fe^{3+} ions occupy the same highly symmetric position $2a$ with virtually unchanged distances between them as for the cubic phase $4a$. The fact that the distances between Fe ions are maintained is also indirectly confirmed by these inset in Figure 2, as mentioned above, — the absence of a jump or inclination change on $\chi(T)$ during phase transition at $T \sim 170$ K.

Since the anisotropy of magnetic properties is not observed experimentally, let us assess the interaction energy for average Θ and λ. The negative interaction may be caused by dipole−dipole exchange interaction. The average paramagnetic temperature $\Theta \approx -0.8$ K that corresponds to $E_{\text{Fe–Fe}} \approx 1.1 \cdot 10^{-16}$ erg.

Dipole−dipole interaction energy for the pair of moments was assessed using the known equation $E_{\text{d–d}} = (gS\mu_B)^2/r^3$ with distances r between the centers of Fe^{3+} atoms. For the cubic phase $Fm3m$, the minimum distance between the nearest neighbors Fe^{3+}, positions $4a$, according to [8] (see also Figure 1), at 290 K is equal to $r = 6.27$ Å. This gives $E_{\text{d–d}}(290\,\text{K}) = 8.72 \cdot 10^{-18}$ erg. For the low-temperature phase in ab plane, $r = 6.154$ Å and $E_{\text{d–d},(ab)}(10\,\text{K}) = 9.23 \cdot 10^{-18}$ erg. In $\{112\}$ type plane, the minimum distance $r = 6.22$ Å and $E_{\text{d–d},\{112\}}(10\,\text{K}) = 8.92 \cdot 10^{-18}$ erg. This corresponds to $T = E_{\text{d–d}}/k_B = 0.072$ K. I.e. dipole−dipole interaction is far from completely explains the obtained paramagnetic Curie temperatures ($\Theta \approx -0.8$ K) and respective energy $E_{\text{Fe–Fe}} \approx 1 \cdot 10^{-16}$ erg.

Indirect exchange interaction between 12 nearest neighbors Fe^{3+} may be performed in chains Fe−F−K−F−Fe. It is negative for linear bonds. probably, at least geometrical frustration is present. In addition, the paramagnetic temperature (and the ordering temperature equal to it according to the simple model) is very low, the ligand — cation excitation energies for F and K are also unknown. For such systems, calculation and even assessment are rather difficult. This is a separate problem. We shall limit ourselves to the experimental result: $E_{\text{Fe–Fe}} \approx 10^{-16}$ erg.

6. Conclusion

Magnetic properties of the Rb_2KFeF_6 elpasolite crystal were studied within 1.8−300 K in magnetic fields H up to 90 kOe. The crystal is a paramagnet with minor negative interaction between Fe^{3+} ions. The temperature dependence follows the Curie−Weiss law with paramagnetic Curie temperature $\Theta \approx -0.8$ K. the effective magnetic moment of Fe^{3+} atom is $\approx 5.9\,\mu_B$. The dependence of the magnetization on the magnetic field is described by the Brillouin function with effective field with negative interaction constant. At $T \approx 170$ K, kind I structural phase transition reveals.

Acknowledgments

The authors are grateful to M.S. Pavlovsky for discussions.

Funding

The study has been performed within the state assignment of the Institute of Physics, Siberian Branch of RAS. Some magnetic measurements (PPMS-9) system have been performed using the equipment of the Krasnoyarsk Regional Center for Collective Use, Krasnoyarsk Scientific Center, Siberian Branch of the Russian Academy of Sciences.

Conflict of interest

The authors declare that they have no conflict of interest.

References

[1] I.N. Flerov, M.V. Gorev, K.S. Aleksandrov, A. Tressaud, J. Grannec, M. Couzi. Mater. Eng. Sci. R **24**, *3*, 81 (1998).

[2] B.V. Beznosikov, K.S. Aleksandrov. Kubicheskie galoidnye el'pasolitopodobnye kristally. Preprint № 798F Institut pgiziki SO RAN, Krasnoyarsk (2000) 44 p. (in Russian).

[3] R. Haegele, W. Verscharen, D. Babel. Z. Naturforsch B **30**, *3*, 462 (1975).
[4] A. Tressaud, S. Khaïroun, J.P. Chaminade, M. Couzi. Phys. Status Solidi A **98**, *2*, 417 (1986).
[5] M. Couzi, S. Khaïroun, A. Tressaud. Phys. Status Solidi A **98**, *2*, 423 (1986).
[6] S. Khaïroun, A. Tressaud, J. Grannec, J.M. Dance, A. Yacoubi. Phase Transitions **13**, 157 (1988).
[7] L.N. Flerov, M.V. Gorev. Phys. Solid State **43**, *1*, 127-136 (2001).
[8] S.G. Vasilovski, V.C. Sikolenko, A.I. Beskrovnyi, A.V. Belushkin, I.N. Flerov, A. Tressaud, A.M. Balagurov. Z. Kristallographie S **23**, 467 (2006).
[9] E. Bucher, H.J. Guggenheim, K. Andres, G.W. Hull Jr., A.S. Cooper. Phys. Rev. B **10**, *7*, 2945 (1974).
[10] M.V. Hoehn, D.Q. Karraker. J. Chem. Phys. **60**, 393 (1974).
[11] V.N. Voronov, E.A. Petrakovskaya. Phys. Solid State **55**, *4*, 730-736 (2013).
[12] A.D. Balaev, Yu.V. Boyarshinov, M.M. Karpenko, B.P. Khrustalev. Prib. Tekh. Eksp. **3**, 167 (1985).
[13] J.S. Smart. Effective Field Theories of Magnetism, W.D. Saunders comp., Philadelfia, (1966), 188 p.
[14] Ch. Kittel. Introduction to Solid State Physics, fourth edition, John Wiley, N, Y., (1971).

Translated by E.Ilyinskaya